

Article citation: Hirt C., Guillaume S., Wisbar A., Bürki B. and Sternberg, H. (2010) Monitoring of the refraction coefficient of the lower atmosphere using a controlled set-up of simultaneous reciprocal vertical angle measurements. *Journal of Geophysical Research (JGR)* 115, D21102, doi:10.1029/2010JD014067

Monitoring of the refraction coefficient in the lower atmosphere using a controlled set-up of simultaneous reciprocal vertical angle measurements

Christian Hirt

Department of Geomatics,
HafenCity Universität Hamburg
Hebebrandstr. 1, 22297 Hamburg, Germany

Now at: Western Australian Centre for Geodesy & The Institute for Geoscience Research
Curtin University of Technology, GPO Box U1987, Perth, WA 6845, Australia
Fax: +61 8 9266 2703; Email: c.hirt@curtin.edu.au

Sébastien Guillaume

ETH Zürich, Institut für Geodäsie und Photogrammetrie.
Schafmattstr. 34 CH-8093 Zürich, Switzerland
Fax: +41 44 633 10 66; Email: guillaume@geod.baug.ethz.ch

Annemarie Wisbar

Department of Geomatics,
HafenCity Universität Hamburg
Hebebrandstr. 1, 22297 Hamburg, Germany
Email: a.wisbar@googlemail.com

Beat Bürki

ETH Zürich, Institut für Geodäsie und Photogrammetrie.
Schafmattstr. 34 CH-8093 Zürich, Switzerland
Fax: +41 44 633 10 66; Email: beat.buerki@geod.baug.ethz.ch

H. Sternberg

Department of Geomatics,
HafenCity Universität Hamburg
Hebebrandstr. 1, 22297 Hamburg, Germany
harald.sternberg@hcu-hamburg.de

Abstract

A great deal of empirical studies have investigated the characteristics of terrestrial refraction. However, only few of these are concerned with short-term fluctuations of refraction influences. The aim of the present work is to analyse the short-term characteristics (amplitudes and variations at scales of minutes to hours) of terrestrial refraction in the lower atmosphere around 1.8 m above grass surface. We apply the known method of simultaneous reciprocal vertical angle measurements to derive time series of the refraction coefficient k as a measure for refraction. Our study uses a new set-up of two pairs of total stations for parallel observations of the refraction coefficient along adjacent lines of sight. Such a controlled experiment not only allows the determination of refraction coefficients independently, but also to assess measurement errors from the residuals between refraction coefficient pairs. Over five observation days in summer 2008, a total of 33 hours of parallel observation data of the refraction coefficient were collected at sampling frequencies of 1 min. On one observation day, unique parallel observations of the refraction coefficient along three lines of sight with a total of six total stations were possible. For mostly sunny days, we found wave-like and saw-tooth-like fluctuations of

the refraction coefficient with amplitudes of 1-1.5 at time scales of 10-30 min. On cloudy days, the amplitudes of fluctuations were on the order of 0.5. Our refraction experiments show a variation range of k between -4 and $+16$ near the ground on sunny summer days. This equates to vertical temperature gradients between -0.5 K/m and -0.1 K/m during the day and $1-2$ K/m shortly after sunset. Cloud cover reduces the variability of k to a range of -2 to $+5$. Our results show that the frequently used Gaussian refraction coefficient of $+0.13$ is not suited for describing refraction effects in the lower atmosphere. As a conclusion, our results may be helpful to better assess the role of refraction in near-ground precision surveys, such as geometric levelling or trigonometric heighting.

1 Introduction

The term atmospheric refraction denotes the effects of the atmosphere on the geometry (curvature) of the path and the velocity of electromagnetic waves. Atmospheric refraction is caused by variations in the refractive index along the path of light, which depend on the physical state of the atmosphere [e.g. *Torge*, 2001]. Different categories are used in the literature to describe the curvature effects of the atmosphere on a path of light between an observer and target [cf. *Thomas and Joseph*, 1996]. The term *astronomical refraction* is used to describe the ray-bending effects for the case when the observer (e.g., with a telescope) is inside Earth's atmosphere and the target (e.g., star or planet) is outside [Young, 2006]. Opposed to this, *terrestrial refraction* denotes cases where both the observer and target are inside the Earth's atmosphere [e.g., *Brocks* 1939; *Hübner*, 1977]. If the path of light travels through the lower atmosphere (i.e. commonly found with near-ground geodetic measurements), terrestrial refraction is also called *geodesic refraction*, cf. *Thomas and Joseph* [1996] or *levelling refraction* [e.g., *Holdahl*, 1981]. The present paper is concerned with terrestrial refraction in the lower atmosphere.

In geodesy, the *coefficient of refraction* k represents a common way to quantify terrestrial refraction. It may be defined as the ratio of the radius of the Earth R and the radius of line-of-sight r , i.e. the radius of a circular arc used as mathematical model to approximate a complex curved path of light [e.g., *Brocks*, 1950a; *Kahmen and Faig*, 1988]. Based on reciprocal vertical angle measurements near Hannover (Germany), Carl Friedrich Gauss found an average value of the refraction coefficient k of approximately $+0.13$ [e.g., *Brunner*, 1984]. The Gaussian value of k is well known to the surveyor as a frequently used standard value of terrestrial refraction.

The Gaussian refraction coefficient, though often suitable to describe refraction effects well above the ground, is *not representative for the lower atmosphere* [e.g., *Brocks* 1950a, 1950b; *Bomford*, 1980]. This region involves the surface layers to a height of about 30 m [Webb, 1984] and, importantly, includes the near-ground domain in which optical geodetic measurements are often carried out (e.g., geometric levelling in general and trigonometrical heighting in flatter regions). Here, the temperature of the air strata, particularly its vertical temperature gradient, is strongly influenced by daily variations in the surface temperature. This may result in either negative and positive values of the refraction coefficient k near the ground with differences to the Gaussian value as large as two orders of magnitude [e.g., *Brocks*, 1950a, 1950b; *Hübner*, 1977; *Eschelbach*, 2009].

Most past empirical works concerned with investigation of terrestrial refraction [e.g., *Angus-Leppan*, 1968; *Hübner*, 1977; *Kharaghani*, 1987, cf. section 2 for a more detailed review] are either based on temperature gradient measurements or visually performed vertical angle measurements which were taken at rates of say 1 or 2 observations per hour, or even less. Such sampling rates do not provide insight into the *short-term fluctuations* (i.e., the variations at time scales of minutes) of the refraction coefficient. By now, only a few studies relate to short-term fluctuations of terrestrial refraction. For example, time series of continuous vertical temperature gradients [direct, e.g., *Hennes*, 2006, and indirect, e.g., *Flach*, 2001] have been published which could be used for analysis of short-term variations in the refraction coefficient. *Kabashi* [2003] derived high-resolution time series of the refraction coefficient over water from automated zenith angle measurements with video theodolites. However, short-term fluctuations of the refraction coefficient in the lower atmosphere over various types of terrain like grass, gravel or bitumen are not addressed much in the recent literature.

The aim of the present work is to analyse the time behaviour of the refraction coefficient under different weather conditions over grass surface at about 1.8 m height. Such conditions are fairly representative for many geodetic measurements near the ground. We apply the method of simultaneous reciprocal vertical angle measurements

(section 3) using high-precision motorized tachymeters with automatic target recognition modules, at high sampling frequencies of 1 observation per minute (section 4). Our study focuses on the fluctuations of the refraction coefficient at time scales of few minutes to hours and examines the variation range in the course of the day. Very short-periodic fluctuations (at scales below 1 min) are not addressed here.

We deployed a controlled set-up of two pairs of total stations observing the refraction coefficient along two adjacent lines of sight. Over five observation days in summer 2008, a total of 33 hours of parallel observation data of the refraction coefficient were collected. On one observation day, unique parallel observations of the refraction coefficient along three lines of sight with a total of six tachymeters were possible (section 5). On the one hand, the parallel and synchronized use of two (or even three) pairs of total station allows us to determine the refraction coefficient independently; on the other hand measurement errors may be assessed from the residuals between refraction coefficient pairs by assuming very similar refraction influences along adjacent lines of sight (section 6).

The importance of refraction research is related to the fact that atmospheric refraction is a main source of error in many geodetic measurements [e.g., *Hennes, 2002, Ingensand, 2008*]. Refraction research not only aims at measuring and modelling of refraction influences, but also contributes to a better understanding of physical processes such as temperature distribution and heat transfer in the atmosphere [e.g., *Geiger et al., 2009*]. Atmospheric refraction, expressed in our study in terms of the refraction coefficient is undoubtedly a key physical effect which is of interest to meteorologists and geodesists. Based on controlled experiments, the present study offers new knowledge on the amplitudes and variability of refraction near the ground. Our experiments yield refraction coefficients which are related to (integral) vertical temperature gradients. These are important parameter to characterize the physical state of atmospheric air strata, allowing interpretation of heat transfer effects near the ground (section 6).

Further to studies dealing with analysis of the characteristics of the refraction coefficient (section 2), past refraction research placed a focus on the development of methods for the *correction* of refraction effects using temperature gradient measurements, turbulence measurements or dual-wavelength instrumentation [for a description and a review of these methods see, e.g., *Brunner, 1984; Böckem et al., 2000; Weiss et al., 2001; Ingensand, 2008*]. The present study is concerned with investigating refraction of the *lower atmosphere* in the *vertical direction*. For an analysis of atmospheric refraction in the horizontal direction (aka lateral refraction), which is relevant to high-precision direction measurements, we refer to, e.g., *Korritke [1992]*, and *Wilhelm [1994]*.

2 Fundamentals and past studies

For a better understanding of refraction effects in the lower and higher atmosphere and the results of our study, some selected aspects of terrestrial refraction will be dealt with first. These include the definition of the refraction coefficient and its relationship to the vertical temperature gradient as well as typical characteristics of terrestrial refraction in different parts of the atmosphere, presented here with some simplifications. We follow a frequently used model concept that subdivides the atmosphere into three different regions, i.e. the *higher, intermediate* and *lower atmosphere* [*Brocks, 1948; Wunderlich, 1985*].

Without claiming completeness, an overview of past works concerned with refraction coefficient determinations is given, in order to exemplify typical magnitudes of the refraction coefficient. The mathematical relations among the refractive index and ray-bending effects are omitted; instead we refer to the literature [e.g., *Jordan et al., 1956, p. 410 ff; Bomford, 1980, p. 234 ff; Torge, 2001, p. 119 ff*]. The examples compiled next will demonstrate on the one hand the variety of parameters (e.g., weather, ground clearance, type of terrain) which the refraction coefficient depends on. On the other hand, they will illustrate the possible variation range of the refraction coefficient encountered in practice.

2.1 Coefficient of refraction

This study uses the coefficient of refraction k defined as ratio between the radius of the Earth R and radius of the line-of-sight r [e.g., *Brocks*, 1950a; *Kahmen and Faig*, 1988; *Schofield and Breach*, 2007]:

$$k = R/r. \quad (1)$$

This definition is based on a circular arc used to model the often irregularly curved path of light [*Kahmen and Faig*, 1988]. For the Gaussian refraction coefficient k of +0.13 [e.g., *Brunner*, 1984] and a mean Earth radius $R = 6370$ km, the average refraction radius of the circular path of light is about 49,000 km. The positive sign of the refraction coefficient indicates a convex shape of the ray of light, i.e. it follows the Earth's curvature. In the literature [e.g., *Bomford*, 1980], sometimes a second definition for the refraction coefficient is found, that is not based on the ratio of radii but on the ratio between the geocentric angle and the refraction angle. This second definition is not used here.

An essential finding of past research efforts is that the refraction coefficient k and vertical temperature gradient are directly related to each other [e.g., *Brocks*, 1939]. The refraction coefficient of a particular point, in the literature commonly referred to as local refraction coefficient and denoted with χ , is connected to the vertical temperature gradient $\partial T/\partial z$ [K/m] using [e.g., *Bahnert*, 1987; *Joeckel et al.*, 2008]:

$$\chi = 503 \frac{p}{T^2} \left(0.0343 + \frac{\partial T}{\partial z} \right) \quad (2)$$

where p is the pressure [HPa] and T temperature [$^{\circ}$ K]. The local refraction coefficient χ is essentially a function of the temperature gradient $\partial T/\partial z$, and depends only slightly on pressure p and temperature T [*Wunderlich*, 1985]. Temperature gradients allow modelling and reducing vertical refraction influences in surveying [e.g., *Brocks*, 1939; *Heer and Niemeier*, 1985; *Kharaghani*, 1987; *Hennes*, 2002; *Ingensand*, 2008].

2.2 Refraction and temperature gradient of the intermediate and higher atmosphere

For the *higher atmosphere*, some 100 m above the ground and higher, the vertical temperature gradient is fairly independent of the temperature of Earth's surface. The vertical temperature gradient $\partial T/\partial z$ is about -0.006 K/m, i.e., a temperature decrease of 6 K per km height difference [*Bomford*, 1980; *Torge* 2001]. For example, the parameters $p = 1013$ HPa, $T = 288.15$ $^{\circ}$ K (= 15 $^{\circ}$ C) and $\partial T/\partial z = -0.0060$ K/m yield a local refraction coefficient χ of +0.17. The *intermediate atmosphere*, about 20-30 m to some 100 m [cf. *Webb*, 1984; *Wunderlich* 1985], is weakly influenced by the temperature of the surface and characterized by temperature gradients frequently of about -0.01 K/m, cf. *Bomford* [1980]. This gradient equates to a refraction coefficient of +0.15. Also, the Gaussian refraction coefficient of +0.13 refers to the intermediate atmosphere and is appropriate for dry adiabatic conditions.

Several studies have observed refraction coefficients of the *intermediate* and *higher atmosphere*. For the Nanga Parbat region (Himalaya Mountains) *Brocks* [1949] computed refraction coefficient values between +0.10 and +0.12 based on temperature gradients. *Mavridis and Papadimitriou* [1973] reported values of the refraction coefficient varying from +0.12 to +0.20, as obtained from vertical angle measurements between two hills in Greece. The results of these indicate fairly small variability of k in regions well above the surface.

2.3 Refraction and temperature gradient of the lower atmosphere

In contrast to the higher and intermediate atmosphere, the thermal characteristics of the air strata of the *lower atmosphere* (lowest 20-30 m) are strongly subjected to the varying thermal properties of the surface [e.g., *Angus-Leppan*, 1968]. In essence, two processes of heat transfer govern the temperature gradients occurring in this region [e.g., *Kukkamäki* 1979, *Geiger et al.*, 2009]:

- (1) Over the day, sun radiation is being absorbed by Earth's surface. The warm terrain, in turn, heats up the lowest atmospheric layers, resulting in negative vertical temperature gradients, and turbulent

motions of air (convection), which are known to the geodetic practitioner as image dancing or scintillation. For example, a gradient $\partial T/\partial z = -0.5$ K/m, derived from practical temperature measurements by *Hennes* [2006], translates to a local refraction coefficient $\chi = -2.9$ [equation 2]. Compared to the Gaussian value of +0.13, this describes not only a stronger, but also a concave curvature of the path of light, i.e. opposite to Earth's curvature.

(2) In the evening, the Earth's surface normally cools off, faster than the overlaying air strata. Usually, this results in strong positive gradients $\partial T/\partial z$ [*Angus-Leppan*, 1968]. Cloud cover attenuates the heat transfer from the sun and, hence, from the ground, thus leading to smaller absolute values of the temperature gradients and refraction effects in the course of a day.

Refraction in 1-3 m height

Brocks [1950b] used sets of temperature measurements for computing vertical temperature gradients at different heights and converted these to local refraction coefficients. For ground clearances of 1–3 m, he showed that the refraction coefficients may exhibit extreme values between -3.5 and $+3.5$. *Angus-Leppan* [1968] utilized temperature gradient measurements as well as a special reciprocal levelling set-up for refraction studies, yielding refraction coefficients between -0.5 to -4 over grass and bitumen surfaces. *Hübner* [1977] deployed a laser beam set-up to show refraction coefficients varying between -4 and $+6$ for a height of 1.5 m above sunny grass surfaces. By means of temperature measurements, *Kharaghani* [1987] obtained temperature gradients varying between -0.4 K/m and $+0.2$ K/m in 1.5 m height over different surface types, corresponding to refraction coefficients roughly between -2 and $+1$. These past studies indicate extreme values of the refraction coefficient of -4 and $+6$ for ground clearances that are typical for near-ground surveying.

Refraction below 1 m height

Brocks [1950b] demonstrated that refraction effects in the lower atmosphere generally multiply with decreasing height. This is because heat transition from the Earth surface is the stronger, the less distant the atmospheric layers are. Therefore, the largest absolute values of temperature gradients are to be expected immediately above the ground. Based on temperature measurements, *Brocks* [1950b] computed possible variations of the refraction coefficient between -47 and $+20$ directly above the ground. Close to the ground in 50 cm height, refraction coefficients were observed to range between -8 and $+16$ on sunny days, cf. *Hübner* [1977]. *Kharaghani* [1987] showed extreme values of refraction coefficients of about -6 to -10 at heights of a few tenths of a metre above the ground. In geodetic practice, however, ground clearances of 50 cm and less are generally avoided.

Refraction over ice and water

Further studies are concerned with the analysis of refraction over ice and water. Both surfaces significantly differ from vegetated ground in terms of their thermal storage properties, usually resulting in an amplification of refraction effects. *Stober* [1995] determined refraction coefficients between 0 and $+2$ from vertical angle measurements for ground clearances between 0.5 m and 4 m over an ice-field in Greenland. *Angus-Leppan* [1968] used reciprocal levelling to measure refraction coefficients in Alaska. He reported a variation of k over ice between -14 and $+10$ for line of sights 1.6 m above the surface. *Kabashi* [2003] obtained refraction coefficients from $+1$ to $+18$ from reciprocal vertical angles for a line of sight about 5 m over water.

3 Methodology

3.1 Mathematical model

The method of simultaneous reciprocal vertical angle measurements is described in the literature by various authors, e.g., *Jordan et al.* [1956], *Bomford* [1980], *Kahmen and Faig* [1988], *Schofield and Breach* [2007], and *Tsoulis et al.*, [2008]. The main application of reciprocal vertical angle measurements is the determination of

height differences [e.g., *Hirt et al.*, 2008], whereby the refraction coefficient k is obtained as a by-product. With vertical angle measurements z_1 and z_2 [°] taken at the endpoints P_1 and P_2 by means of total stations (tachymeters), the refraction coefficient is computed from [*Bahnert*, 1986a; *Kahmen and Faig*, 1988]:

$$k \approx 1 - \frac{z_1 - z_2 - 180}{180/\pi} \cdot \frac{R}{S} \quad (3)$$

with R the radius of the Earth and S the distance between P_1 and P_2 (Figure 1). Importantly, k derived from reciprocal vertical angle measurements is a *mean* value along the sight between P_1 and P_2 and does not refer to a particular point. In order to contrast local refraction coefficients χ from temperature gradients, the term *effective refraction coefficient* is sometimes used to denote k -values from reciprocal sights [e.g., *Bahnert*, 1986a; *Joeckel et al.*, 2008]. Equation 3 is based on the assumption of a symmetrical path of light which is approximately fulfilled when the terrain profile and atmospheric conditions between P_1 and P_2 are fairly uniform [*Kahmen and Haig*, 1988]. A second underlying assumption in equation (3) is circularity of the path of light. This strictly holds only for the vertical temperature gradient $\partial T/\partial z$ of -0.0171 K/m [*Wunderlich*, 1985]. Here we stay consistent with previous works on refraction analysis by using equation (3), thus assuming a circular arc as a geometrical model for the refracted path of light. The rigorous analysis of the actual geometry of the refracted path of light as a function of the temperature gradient is beyond the scope of this study.

Equation (3) is valid for horizontal sightings; the mathematical relations for inclined terrain are given by, e.g., *Wunderlich* [1985] and *Tsouliis et al.*, [2008]. We acknowledge that the derivation of equation (3) is based on some approximations while an exact algebraic solution has been derived in *Tsouliis et al.* [2008]. According to this reference, the difference between the approximate equation (3) and the exact algebraic solution is zero for horizontal sights. This is the case with our field experiments.

3.2 Error analysis

Bahnert [1986b] discussed the accuracy of refraction coefficients from simultaneous reciprocal zenith observations as a function of the accuracy of all quantities (z_1 , z_2 , S , R) appearing in equation (3). The standard deviation σ_k of the refraction coefficient essentially depends on the accuracy σ_z of the zenith angle measurements while those of the distance between P_1 and P_2 and the Earth's radius R are negligible in practice. Assuming equal standard deviations σ_z for the vertical angles z_1 and z_2 , then the application of the propagation law of variances yields:

$$\sigma_k = \sqrt{2} \frac{\partial k}{\partial z} \sigma_z \quad (4)$$

with

$$\frac{\partial k}{\partial z} = \frac{R}{S} \frac{\pi}{180} \quad (5)$$

Figure 2 shows the standard deviation σ_k of the refraction coefficient as a function of typical accuracy classes σ_z of total stations (1", 2", 3" and 5") and different distances S between the observation points P_1 and P_2 . An inverse relation between the accuracy σ_k and the distance S is visible, i.e. the larger the spacing between the endpoints, the more accurate is the determination of k [cf. *Ramsayer*, 1979]. For example, in order to attain an accuracy level σ_k of 0.2 for the refraction coefficient, the endpoints should be at least 700 m apart when a 1 mgon (approximately 3") total station is being used. A discussion of the accuracy level of the practical refraction coefficient measurements is given in section 6.

4. Instrumentation

For the practical field experiments, TCRP 1201(plus) total stations by Leica Geosystems and the Daedalus measuring system by ETH Zurich were used. In the following, both systems are briefly characterized with focus on the different techniques used for automatic angle observations (automatic recognition and measurement of the target points).

4.1 Leica TCRP 1201

The TCRP 1201 total station (Figure 3, left) is motorized and has Leica automatic target recognition (ATR) technology [e.g., Haag *et al.*, 1997; Zeiske, 1999]. The accuracy of the TCRP 1201 vertical angle measurements taken in two telescope positions (face left and face right) is specified to be 1" (0.3 mgon).

Leica ATR utilizes a focused laser beam (infra-red) which is emitted through the telescope of the total station. The laser beam is reflected back by the retro-reflector and then imaged onto a charge-coupled device (CCD) sensor inside the total station. The position of the back-reflected laser beam on the CCD, determined by the centre-of-mass algorithm [e.g., Auer and van Altena, 1978], is a measure for the direction differences of the target with respect to the optical axis of the total station (see, e.g., Haag *et al.*, [1997], Kirschner and Stempfhuber [2008], and Wasmeier [2009] for more details). Together with the motorization, the built-in ATR modules enable the automated acquisition of time series of vertical angle data. A main benefit of ATR is a more constant measurement precision over the day and more consistent results [Haag *et al.*, 1997]. A drawback, however, is that the ATR zero offset (i.e., the angle between the telescope axis and the ATR axis) does not cancel out in two telescope positions [e.g., Leica, 2003]. Therefore, the use of ATR requires thorough calibration.

The calibration of ATR is based on manual pointings to the retro-reflector, which are being compared against those of the ATR module. The angular differences obtained in the horizontal and the vertical direction represent the ATR calibration parameters, subsequently applied as corrections to each angle reading [e.g., Wasmeier, 2009]. Any residual errors of the calibration parameters (e.g., random errors inherent in the calibration parameters or variation of the calibration parameters with time or temperature) cause a deviation with respect to the "true", albeit unknown values of the calibration parameters. Any deviation therefore reduces the angle accuracy in a systematic manner (see section 6). This is of particular relevance for high-precision vertical angle measurements in refraction determination.

In order to perform angle observations *simultaneously* and *reciprocally*, stable base plates were attached to the tripod, so as to accommodate both the total station and the retro-reflector (corner cube) being the target point (see Figure 3 left). The small vertical height offset between the centre of the reflector and the horizontal axis of the total station can be accurately (0.5 mm standard deviation) determined using a precision level and applied as an angular correction [Hirt *et al.*, 2008]. For the steering of the total stations (execution of measurements at equidistant epochs and data storage), laptop computers were used with control software developed at HafenCity University (HCU) Hamburg. The synchronization of the reciprocal measurements was achieved using the internal laptop clocks, which were compared and adjusted before, and, in order to reduce the impact of clock drifting, occasionally during the measurements. The estimated precision of synchronization is 1-2 s.

4.2 Daedalus

The Daedalus measuring system (Figure 3, right) has been developed at ETH Zürich [Guillaume and Bürki, 2008]. It was originally designed for automatic low-cost astrogeodetic measurements, but it is also applicable for reciprocal zenith angle measurements. The system consists of two Leica TCA1800 total stations [e.g., Haag *et al.*, 1997], where each ocular is replaced by a triggerable CCD camera. A slightly divergent lens is placed in front of the objective in order to translate back the image plane, created by the optical system of the total station, in the plane of the CCD chip. The chip size is 1024x768 pixels. With a pixel size of 4.65 micrometer, the pixel

resolution is 4 arc seconds and the field of view is $1.1^\circ \times 0.8^\circ$. For terrestrial observations, usually well-defined illuminated targets (lamp, diodes) are used.

The correspondence between angles and pixels extracted from the CCD is obtained from a modified affine transformation. The six parameters of the transformation are determined by an in-situ automatic calibration procedure (without human intervention) by measurements of a well defined and extractible object, measured in different directions. The automatic measurement of target points can be done with two different methods. The first method is based on the recognition of a pre-defined template (cross-correlation, cf. *Lewis [1995]* and least-squares template matching, cf. *Berger [1998]*). The second method measures spot-shaped objects by a centre-of-mass determination [e.g., *Auer and van Altena, 1978*]. Both methods are capable of measuring the target with an accuracy of better than 0.1 pixels or 0.4 arc seconds, respectively.

For simultaneous reciprocal observations, sightings are made directly on the line of sight of the second total station (Leica TCA 1800). This is achieved by means of a ring of four light emitting diodes (LEDs), symmetrically placed around both objectives (cf. Figure 3, right). With the target centred to the lens, the vertical height offset (between target and horizontal axis of the total station) is zero for horizontal sightings. The centre-of-mass method is used in order to perform observations free of any systematic errors, e.g., due to template definition. The timing is realized with a GPS (Global Positioning System) receiver [e.g., *Seeber 2003*] integrated in the Daedalus system. The exposure time of the CCD target images may vary between 1 and 30 ms. Depending on the light conditions, the exposure time is chosen in such a way that yields the best signal-to-noise ratio (i.e., a dark background and a bright target picture on the CCD).

There are some advantages of the Daedalus automatic targeting over the Leica ATR technique. First, the Daedalus automatic targeting system is passive as it does not use a laser. Therefore, as opposed to the standard Leica ATR, no light is emitted and back-reflected by a corner cube, which may be a further source of possible errors. Second, the distance between the stations can be increased significantly up to several tens of kilometres using bright targets. Third, the Daedalus calibration of the CCD is more rigorous than the standard Leica ATR due to the higher-order calibration model applied. Other than Daedalus automatic targeting, the calibration process of the Leica ATR is operator-dependent and only provides estimates of the offsets for the horizontal and for the vertical component, respectively, while a scale factor or rotations cannot be taken into account. Fourth, Daedalus two face measurements eliminate residual systematic errors of the automatic targeting.

5 Field experiments

We selected a grassland area near Großmoor/Seevetal, south of Hamburg, as the site of our field experiments. The test area is completely even and level, allowing us to meet the requirements for the application of equation (3), namely a uniform type of terrain. Further to this, the selected site is large enough to realize long distances of several 100 m between the stations which is required for precise determination of refraction effects (cf. section 3.2 and Figure 2).

Over five days in August and September 2008, we used two pairs of total stations in parallel operation for simultaneous reciprocal vertical angle measurements (Table 1). The TCRP1201 total stations of each pair were set up with a spacing of about 800 m and a parallel displacement of about 12 m between the lines (cf. Figure 4). The first parameter was chosen to stay within the working range of ATR (specified to 1000 m). The latter value was chosen so as to avoid interferences of the automatic target recognition of adjacent total stations. Such a controlled field experiment yields two refraction coefficient values per measuring epoch. The ground clearance of the two lines of sight was approximately 1.8 m which we consider to be representative for many optical geodetic measurements near the ground. Subsequently, we denote instruments and results of the northern line of sight with A and those of the southern line with B (Figure 4).

It was decided to measure the vertical angles always in two telescope positions (dual face observations) in order to reduce the impact of instrumental zero offset variations (with time, e.g., originating from temperature changes) on our measurements. These include a.) the zero offset of the *vertical circle (vertical index offset)*, and,

b.) the zero offset of the *tilt sensors (compensator index offset)*. See, e.g., *Kahmen and Faig* [1988], and *Schofield and Breach* [2007] for more details on instrumental zero offset errors.

With the described TCRP 1201 equipment and chosen set-up, synchronized reciprocal measurements could be reliably performed at sampling rates of 1 min (30 s per face). Test measurements using higher sampling rates (e.g. 10 s or 15 s per face), exhibited numerous data gaps under unfavourable conditions (i.e., strong scintillation during sunny weather), requiring more time to accomplish the automatic targeting. Always four simultaneously observed zenith angles are required to compute the difference between pairs of refraction coefficients. As already one single missing registration prevents such a computation, the reliable availability of data was given priority over a higher sampling rate. Therefore, a sampling rate of 1 min (30 s per face) was used in our field experiments.

Table 1 gives an overview about the data sets collected with the four TCRP1201 total stations over five days. The data sets cover different weather conditions (two mostly sunny and three cloudy days) and a total of about 2000 epochs (33 h net observation time). The majority of the vertical angle measurements was performed in two hour sessions, interrupted for calibration of the ATR zero offset (section 4) of the instruments.

On the 09.09.2008, unique parallel observations of the refraction coefficient along three lines of sight with a total of six tachymeters were performed. Together with the two TCRP 1201 tachymeter pairs, the ETH Zurich Daedalus measurement system (section 4.2) collected about 4 hours of vertical angle readings at sampling frequencies of 20 s (10 s per face). The arrangement of the measurement systems on 09.09.2008 is depicted in Figure 4. The bottom line of Table 1 shows the characteristics of the Daedalus measurements.

6 Results and discussion

All TCRP1201 vertical angles were centred to the horizontal axis of the opposite tachymeter using measurements of the vertical offset between the centre of the reflector and the horizontal axis of the total station. For the Daedalus observations, such a reduction was not required (section 4.2).

The vertical angle measurements of each line of sight (A and B) were then used for the computation of refraction coefficients k [equation (3)]. The resulting time series of the refraction coefficient k – as obtained from tachymeter pairs A and B – are depicted in Figure 5a-e while Figure 5f shows the results for a selected time window of 6 hours on 09.09.2008 (sunny day). The bottom part of each panel shows the differences Δk between the parallel observations at same epochs. For better interpretation of the results, a second axis was added to each plot, indicating the vertical temperature gradient $\partial T/\partial z$. The temperature gradients are computed based on equation (2) assuming that the gradient is representative along the line of sight. The k -values are plotted as a function of the time CEST (Central European Summer Time).

6.1 TCRP1201 results

The comparison of the time series of the refraction coefficient k (Figure 5) indicates a good agreement between lines of sight A and B. It is seen that the short-term (5-60 min) variations and those at scales of some hours were similarly captured by the two pairs of TCRP1201 measurement systems. This is a confirmation of very similar atmospheric conditions, and, hence, similar refraction influences along the two lines of sight, as assumed prior to the field observations. Measurement noise, e.g. due to scintillation, is visible at very short time scales below 5 min (cf. Figure 5).

For a mostly sunny day (09.09.08), Figure 5 (e,f) exhibits several wave-like and saw-tooth-like fluctuations of k with amplitudes of 1.5 at time scales of 15-20 min, with the k -values ranging mostly between 0 and -3.5 . The latter value corresponds to a radius of the line-of-sight r of about 1770 km (equation 1) and a concave path of light, i.e. with the centre of the ray of light bended towards the Earth. These fluctuations are attributed to isolated clouds reducing the heat transfer from the sun. The vertical temperature gradients range, indirectly obtained from equation 2 is found to extend from 0 K/m to -0.6 K/m. This is in good agreement with gradients obtained from

direct temperature measurements in another test area under similar conditions (-0.2 K/m to -0.6 K/m, cf. *Hennes*, [2006]).

For a predominantly cloudy summer day (03.09.08), Figure 5d shows refraction coefficient values ranging between -2 (noon and early afternoon) and about $+1$ in the evening hours. Variations of the refraction coefficient are found to occur on time scales from hours to several minutes, e.g., δk of $+1.5$ between 12.00 h and 13.00h, δk of $+2$ between 14.00 h and 14.15 h and δk of -1 between 14.15 h and 14.20. Strong variations of k are observed on 09.09.08 (mostly sunny day) with k values between 0 and -3.5 (10.00h and 17.00h) and steadily increasing to values as large as $+13$ in the evening hours (Figure 5e). Such an extreme value of k equates to a radius of the line-of-sight r as small as 490 km with the path of light bended with Earth's curvature.

The behaviour of the indirectly observed temperature gradients on the sunny days 30.08. and 09.09.08 conforms to the thermal processes of the lower atmosphere, as described in Sect. 2.3. During the day, temperature gradients of -0.1 K/m to -0.5 K/m reflect the warming up of the lowest atmospheric layers over heated ground. In the evening hours, the situation reverses with temperature gradients as high as 1-2 K/m caused by the warmer air strata laying over a cooler surface [cf. *Kukkamäki*, 1979]. As seen from Figure 5, cloud cover clearly attenuates these processes.

6.2 Comparison of TCRP1201 and Daedalus results

Figure 6 shows the refraction coefficient k , as observed with the three pairs of tachymeters TCRP 1201 A, TCRP 1201 B and Daedalus between 16.30 h and 21.00 h on 09.09.08 (cf. Figure 4 for the arrangement of instruments along the three lines of sight). The illustration reveals a good agreement among the three sets of parallel observations. Features occurring at times scales of 5 min to hours are similarly contained in the different data sets. The noise level is found to be low during the day (standard deviations (STD) from differences TCRP A – Daedalus and TCRP B – Daedalus of about 0.3), while increasing in the evening hours to a level as large as 0.6 (cf. Table 2). A reasonable explanation for this behaviour is derived from the fact that the strength of atmospheric turbulence is closely related to the vertical temperature gradient and, hence, to the refraction coefficient [cf. *Brunner*, 1979; 1982].

Though the results from this simultaneous refraction experiment along three similar lines of sight are based on the same methodology (vertical angle measurements), the instrumentation is different and operated independently from each other. The most important difference is the different technology used for the targeting (electro-optical infra-red ATR with Leica TCRP 1201 and optical target recognition with Daedalus, as described in section 4). Therefore, we consider the reasonable mutual agreement of the refraction coefficient time series as evidence of the correctness of our results.

It is acknowledged that the different wavelength ranges used by our instrumentation result in differences in the refraction angles and refraction coefficients due to *dispersion*. According to *Böckem* [2001, p. 28], refraction angles differ by about 1/42 (or 2.4 %) for two monochromatic light sources with wavelengths of 430 nm (blue) and 860 nm (near infrared), respectively. With the instrumentation used here (Leica ATR: monochromatic infra-red light and Daedalus: polychromatic visible light, giving a mixed dispersion effect), dispersion does not play a significant role in our comparisons.

6.3 Summary of refraction behaviour

The main result of our study, the refraction coefficient curves for all observation days are shown in Figure 7. The comparison among days with similar weather conditions reveals comparable characteristics at time scales of a few hours. For example, the refraction coefficients on 30.08.08 and 09.09.08 (mostly sunny days) are strongly negative during the day (mostly between -1 and -3). Around 2.5 hours before sunset, refraction continuously increases to the positive range with peaks of about $+12$ to $+16$ equally present in the data around sunset (sunset was on 09.09.08: 19:50 h and 30.08.08: 20:15 h). This equates to large positive temperature gradients of up to $+2$ K/m. The refraction coefficients on cloudy days generally exhibit smaller variations. Over the day, variations of

k mostly between 0 and -2 can be observed while positive values are seen in the evening hours. The lowest variations in k are observed for a rainy observation day (27.08) with oscillations mostly in the order of ± 0.5 .

Despite the coarse agreement of refraction under similar weather conditions, the detailed features unsurprisingly do not compare. For example, the comparison of the short-term oscillations of k reveals rather small amplitudes of 0.25-0.5 (30.08.08) while larger amplitudes of 1.5 are found on the 09.09.08. Apparently, differences in weather conditions (such as varying wind strength or cloud thickness) influence the vertical temperature gradient and, in turn, the refraction coefficient.

6.4 Accuracy aspects - ATR

Despite the overall good agreement among simultaneously observed refraction coefficients in terms of fluctuations and variation range, the detailed inspection of the residuals (bottom part of the six panels in Figure 5) shows the presence of systematic influences on the k -values – instead of randomly scattered differences centred to the zero axis. This is particularly visible from the data acquired on 27.08.08, 30.08.08 as well as 03.09.08 with the systematic displacements of the k -differences from the zero axis ranging between 0.2 and about 0.4. The analysis of the residuals shows nearly constant displacements between the k -values of the two hour sessions with jumps appearing between subsequent sessions. This strongly suggests that the ATR is a possible culprit. Atmospheric influences can be excluded because abrupt jump-like effects are not to be expected, e.g., due to changes in refractivity along adjacent lines of sights.

Between the sessions, the ATR of each of the four TCRP1201 tachymeters was calibrated with meticulous efforts (6-10 exact manual pointings to the retro-reflector). This was done in order to minimize the impact of any changes of the ATR zero offset on the vertical angle measurements over the day (cf. section 4). Both the presence of micro-seismical influences (due to road and railway traffic near our test area) and wind-induced vibrations of the tripods and tachymeters are possible sources of error that might have affected the accuracy of the ATR calibration. Any deviation of the calibrated ATR vertical offset from its true value (i.e., the exact angular difference between the optical and ATR axis) biases the vertical angle readings and causes the vertical angles from dual face observations to be either systematically too large or small. The different displacements between the k -determinations from both lines of sight reflect the accumulation of any errors in the ATR vertical offset calibration of the four TCRP 1201 tachymeters.

In order to relate the observed displacement of the k -differences to the vertical angle measurements, it is derived from equation (3) that a vertical angle bias of 1" equates to a bias in k of 0.038. Consequently, a displacement of the k -residuals of about 0.4 equates to an accumulated bias of the vertical angle measurements of about 10" (= 3 mgon). In another project (trigonometric height transfer from simultaneous reciprocal measurements across the Elbe river in Hamburg, results unpublished) using the same equipment and same methodology, we observed quite similar ATR calibration influences on our results. This provides some evidence to assess the ATR calibration as a weak link in the refraction experiments. It should be noted that changes in k (and therefore conclusions on the fluctuations) remain unaffected. A further detailed investigation of the ATR calibration, e.g. in terms of stability and accuracy, under different environmental conditions is beyond the scope of the present study and remains as a future task.

6.5 Accuracy aspects – angular measurement precision

An appropriate measure to describe the precision of vertical angle measurements is their *empirical standard deviation*, computed from the variations of the vertical index offset. This measure includes instrumental errors in the vertical angle measurement such as the electronic vertical circle reading, the tilt correction as well as atmospheric turbulences causing apparent short-periodic movements of the target (aka scintillation or image dancing). From the variations of the vertical index offsets of the four TCRP instruments over the day, the empirical standard deviation of the vertical angles is found to vary between 1.3"-2.8" on cloudy days and 3.4-3.8" on sunny days. The larger values on sunny days are due to increased atmospheric turbulence [cf. Brunner, 1982], acting as an additional source of uncertainty in the vertical angle measurements. In comparison to the

instrumental accuracy specification of 1", these figures clearly demonstrate that atmospheric influences place limitations on the precision of vertical angle measurements [cf. Brunner, 1979]. Taking into account the empirical standard deviations of the vertical angles, variance propagation (equation 2) yields standard deviations of k of 0.08-0.15 on cloudy days and 0.19-0.21 for sunny days.

Analysing the differences between the k -values of lines of sight A and B represents an alternative way to determine the precision of the refraction coefficient. Table 3 reports the descriptive statistics of the k -differences for our five observation days. The root mean square (RMS) values reflect the uncertainties of both k -measurements while the standard deviation ($STD = RMS/\sqrt{2}$) of the single values indicates the random errors of a single k -observation. It is seen that the STD values range between 0.22 and 0.50, so exceeding their pre-calculated estimates from equation (2). In order to remove any impact of the ATR calibration on the descriptive statistics, the mean value of the residuals Δk has been subtracted for each session separately (bias fit). From the de-biased statistics (Table 4), the STD values are found to have a range between 0.12 and 0.16 on cloudy days and to be about 0.3 for sunny days.

Taking into account that refraction influences (and hence the refraction coefficients to be expected) are similar, but not exactly the same along both lines of sights, and accounting for small synchronization errors, then the agreement among the STD values and pre-calculated estimates from equation 2 is fairly acceptable. The level of precision (not accuracy) achieved in practise varies between 0.1 and 0.3, which is sufficient for the purpose of our study.

7 Conclusions

This study investigated the fluctuation (short-term variations and variation range) of the refraction coefficient k based on simultaneous reciprocal vertical angle measurements. Over a total of five days, a controlled set-up of two pairs of Leica TCRP 1201 tachymeter was used in parallel operation for vertical angle measurements. A third pair of tachymeters (Daedalus system based on Leica TCA 1800 tachymeters) was used along with the TCRP 1201 instruments for simultaneous k -measurements along three densely spaced lines of sight.

Our refraction experiments, carried out across homogeneously vegetated grassland with a ground clearance of about 1.8 m (i.e., an often used working height in surveying), showed a range of k between -4 and $+16$ for sunny summer days. Expressed in terms of vertical temperature gradients, this corresponds to variations of -0.5 K/m to -0.1 K/m during the day and values as large as $1-2$ K/m shortly after sunset. Cloud cover reduces the variability of k to a range of -2 to $+5$. Our results corroborate that the Gaussian refraction value of $+0.13$ is not suited for describing refraction effects in the lower atmosphere.

On the one hand, we consider our results to be a clear confirmation of results obtained in previous studies under similar conditions by Hübner [1977] and Hennes [2006]. On the other hand, our empirical results show that the refraction coefficient k may reach magnitudes as large as $+12$ to $+16$ over grassland at 1.8 m. This clearly exceeds previously published 'extreme values' (e.g., maximum values of $k = +6$ at 1.5 m height over grassland, cf. Hübner [1977]). We acknowledge that surface types like ice or water may even produce larger refraction effects, as described in section 2.

Probably for the first time, near-ground fluctuations of the refraction coefficient k over grassland at time scales of some minutes to 1 hour were investigated. For mostly sunny days, we found wave-like and saw-tooth-like fluctuations of the refraction coefficient with amplitudes of 1-1.5 at time scales of 10-30 min. On cloudy days, the amplitudes of fluctuations were on the order of 0.5, occurring at similar time scales.

The experiment using a unique controlled set-up of four and six tachymeters provided several benefits. On the one hand, they mutually confirmed the findings of our refraction experiment and helped to realistically assess the precision of our k -determinations. On the other hand, they revealed that the TCRP 1201 vertical angle measurements are subject to residual systematic errors which very likely come from the residual errors of the ATR calibration. The ATR calibration needs to be further investigated. An open question is, e.g., how environmental conditions (seismical influences, wind) impact on the accuracy of the ATR calibration

parameters. It should be noted that the analysis of changes of k is unaffected by ATR uncertainties. The results obtained using the Daedalus measuring system by ETH Zurich are considered not to be biased by calibration errors. This is because of Daedalus residual errors of the calibration cancel out in dual face observations, as opposed to those carried out with the TCRP 1201 instruments.

Our refraction experiment was designed to replicate conditions which are frequently found in geodetic practice, i.e., a.) lines of sight passing through the lower atmosphere with a ground clearance of 1.8 m, b.) grassland as a surface vegetation, c.) moderate climate conditions (20-25°C during sunshine, 14-20° under cloud cover). Interestingly, many textbooks [e.g., *Kahmen and Faig*, 1988; *Torge*, 2001; *Kahmen*, 2006; *Witte and Schmidt*, 2006] do not specify the wide range which the refraction coefficient k may vary by under such conditions. Instead, values which are too small are quoted or vague statements are made, leaving open the variation range of k near the ground. An exemption is *Schofield and Breach* [2007], acknowledging variations of k “from -2.3 to 3.5 with value over ice as high as +14.9”, which is a step into the right direction. However, a realistic quantification of the variation range of the refraction coefficient k in the lower atmosphere would be useful to the practitioner. It would help to better assess the role of refraction and its variability near the ground under realistic conditions, in particular on days with strong refractivity such as sunny days.

The present study makes a beginning in investigating the short-term fluctuation of the refraction coefficient k by means of reciprocal vertical angle measurements using automated instrumentation. As further future work, the fluctuations of k could be analysed in the course of the seasons, e.g. observations during summer and winter time, supplemented by an analysis of how geodetic measurements are affected. Further to this, future work could involve simultaneous refraction measurements using different instruments and applying different methods, such as vertical angle measurements along with precision temperature gradient measurements [e.g. *Hennes*, 2006] and scintillometry [e.g., *Flach*, 2001]. This would provide an independent and mutual check on the experiments.

As a further extension of the refraction experiments, meteorological data such as wind speed, wind direction and cloud cover could be automatically acquired with suited meteorological sensors. Importantly, precise cloud cover observations could be related to the variability of the refraction coefficient and the response time of the refraction coefficient could be investigated. The simultaneous sampling of refraction and meteorological data would then allow analyses of the high-frequent fluctuations and deterministic variations of refraction. This would contribute to a better understanding of high-frequent refraction effects in the lower atmosphere.

Acknowledgements

We would like to thank Leica Geosystems (Switzerland) for generously making four TCRP1201 tachymeter available, allowing us to successfully accomplish our refraction project. We are grateful to Fayik Tekin and Svenja Priess for supporting the field observations. Jörg Münchow and Felix Tschirschwitz are thanked for developing the control software. Klaus Mechelke (all HCU Hamburg) helped to compile the field equipment. We thank the reviewers, particularly reviewer #1, for their valuable and encouraging comments on the manuscript and the editor (Sara Pryor) for the handling of the review process.

Bibliography

- Angus-Leppan, P.V. (1969), Surface effects on refraction in precise levelling, *Proceedings REF-EDM Conference 5-8. Nov. 1968*, New South Wales (Australia), Department of Surveying, University of New South Wales, 74 – 89.
- Auer, L. H., and van Altena, W. F. (1978), Digital Image Centering II, *The Astronomical Journal*, 83, 531 – 537.
- Berger, M. (1998), The framework of least squares template matching, *Technical Report Image Science Lab ETH Zurich*, Nr. 180, ETH Zurich. URL: <http://www.vision.ee.ethz.ch/> (accessed 08.02.2010)
- Bahnert, G. (1986a), Refraktion und Refraktionskoeffizient. *Vermessungstechnik* 34(8), 276 – 279.

- Bahnert, G. (1986b), Zur Genauigkeit der geodätischen Refraktionsbestimmung, *Vermessungstechnik*, 34(10), 345 – 348.
- Bahnert, G. (1987), Zur Bestimmung lokaler Refraktionskoeffizienten. *Vermessungstechnik*, 35(1), 14 – 17.
- Böckem, B., P. Flach, A. Weiss, and Hennes, M. (2000), Refraction influence analysis and investigations of automated elimination of refraction effects on geodetic measurements, *Paper presented at XVI IMEKO World Congress 2000, 25-28 Sept. 2000, Vienna.*
- Böckem, B. (2001), Development of a dispersometer for the implementation into geodetic high-accuracy direction measurement systems, *Dissertation ETH Zurich*, Nr. 14252.
- Bomford, G. (1980), Geodesy, Fourth Edition, *Clarendon Press*, Oxford.
- Brocks, K. (1939), Vertikaler Temperaturgradient und terrestrische Refraktion, insbesondere im Hochgebirge, *Veröffentlichungen des Meteorologischen Instituts der Universität Berlin*, Band III(4), 80 pages.
- Brocks, K. (1948), Über den täglichen und jährlichen Gang der Temperatur in den unteren 300 m der Atmosphäre und ihren Zusammenhang mit der Konvektion, *Berichte des Deutschen Wetterdienstes in der U.S. Zone*, Nr. 5, 30 pages.
- Brocks, K. (1949), Die terrestrische Refraktion in polytropen Atmosphären. *Ocean Dynamics* 2(5), 199 – 211.
- Brocks, K. (1950a), Die Lichtstrahlkrümmung in Bodennähe. Tabellen des Refraktionskoeffizienten, I. Teil (Bereich des Präzisionsnivelements). *Deutsche Hydrographische Zeitschrift* 3(3-4), 241 – 248.
- Brocks, K. (1950b), Meteorologische Hilfsmittel für die geodätische Höhenmessung. *Zeitschrift für Vermessungswesen*, (3), 71 – 76, (4), 110 – 116, (4), 145 – 152.
- Brunner, F.K. (1979), Atmospheric turbulence: The limiting factor to geodetic precision, *Australian Journal Geodesy Photogrammetry and Surveying*, 31, 51 – 64.
- Brunner, F.K. (1982), The effect of atmospheric turbulence on telescopic observations, *Bulletin Geodesique*, 56, 341 – 355.
- Brunner, F.K. (1984), Geodetic refraction. Effects of electromagnetic wave propagation through the atmosphere. *Springer Verlag*, Berlin, Heidelberg.
- Eschelbach, C. (2009), Refraktionskorrekturbestimmung durch Modellierung des Impuls- und Wärmeflusses in der Rauigkeitsschicht, *Deutsche Geodätische Kommission*, C 635, München.
- Flach, P. (2001), Analysis of refraction influences in geodesy using image processing and turbulence models, *Geodätisch-geophysikalische Arbeiten in der Schweiz*, Nr. 63, Schweizerische Geodätische Kommission.
- Geiger, R., R.H. Aron, and P. Todhunter (2009), The climate near the ground, Seventh edition, *Rowman & Littlefield Publishers, Inc*, Lanham, MD, ISBN 978-0742555600
- Guillaume S., and B. Bürki (2008), Digital Astrogeodetic Online Observation System Daedalus. User Manual V1.0, Report, *Institut für Geodäsie und Photogrammetrie, ETH Zürich*, Switzerland.
- Haag, R., G. Bayer, M. Zimmermann, and R. Scherrer (1997), Vermessen mit der automatischen Feinzielung des TCA1800 von Leica, *Vermessung, Photogrammetrie, Kulturtechnik* 7/97, 6 pages.
- Heer, R., and W. Niemeier (1985), Theoretical models, practical experiments and the numerical evaluation of refraction effects in geodetic levelling. *Third International Symposium on the North American Vertical Datum NAVD 1985 (21.04-26.04.1985, Rockville, Maryland)*, Springer, Berlin New York, 321 – 342.
- Hennes, M. (2002), Zum Refraktionseinfluss auf terrestrische geodätische Messungen im Kontext der Messtechnik und Instrumentenentwicklung., *Flurbereinigung und Bodenordnung*, 2(2002), 73 – 86.
- Hennes, M. (2006), Das Nivelliersystem-Feldprüfverfahren nach ISO 17123-2 im Kontext refraktiver Störeinflüsse, *Allgemeine Vermessungsnachrichten*, 3/2006, 85 – 94.
- Hirt, C., U. Feldmann-Westendorff, V. Böder, B. Bürki, S. Guillaume, R. Heyen, T. Stelkens-Kobsch, and H. Sternberg (2008), Präzise Höhen- und Schwerefeldbestimmung an Stromübergängen und Meerengen, *Geoinformation in der Küstenzone*, HCU Hamburg, 08.-09.10.2008 (Ed. Traub, K.-P., J. Kohlus and T. Lüllwitz), Points Verlag, Norden Halstad, ISBN 978-3-9812883-0-8, 59 – 72.
- Holdahl, S.R. (1981), A model of temperature stratification for correction of levelling refraction. *Bulletin Geodesique*, 55, 231 – 249.
- Hübner, E. (1977), Einfluss der terrestrischen Refraktion auf den Laserstrahl in bodennahen Luftschichten. *Vermessungstechnik*, 25(10), 349 – 353.
- Ingensand, H. (2008), Concepts and solutions to overcome the refraction problem in terrestrial precision measurement. *Geodesy and Cartography (Geodezija ir Kartografija)*. 34(2). 61 – 65.
- Joeckel, R., M. Stober, and W. Huep (2008), Elektronische Entfernungs- und Richtungsmessung und ihre Integration in aktuelle Positionierungsverfahren. *Wichmann Verlag*, Heidelberg.

- Jordan, W., O. Eggert, and M. Kneissl (1956), Handbuch der Vermessungskunde Band III, *J.B. Metzler'sche Verlagsbuchhandlung*, Stuttgart, 410 – 435.
- Kabashi, I. (2003), Gleichzeitig-gegenseitige Zenitwinkelmessung über größere Entfernungen mit automatischen Zielsystemen, Dissertation, *Technische Universität Wien*, 101 pages.
- Kahmen, H., and W. Faig (1988), Surveying, *Walter de Gruyter*, Berlin, New York.
- Kahmen, H. (2006), Angewandte Geodäsie: Vermessungskunde, 20. Auflage, *Walter de Gruyter*, Berlin, New York.
- Kharaghani, G.A. (1987), Propagation of refraction errors in trigonometric height traversing and geodetic levelling, Technical Report No 132, *Department of Surveying Engineering, University of New Brunswick (UNB)*, Canada.
- Kirschner, H. and W. Stempfhuber (2008), The kinematic potential of modern tracking stations – a state of the art report on the Leica TPS 1200+, Paper presented at *1st International Conference on Machine Control and Guidance 2008*, 10 pages.
- Korritke, N. (1992), Horizontalrefraktion in langen Tunneln, *XI. Internationaler Kurs für Ingenieurvermessung*, 21.-26. Sept. 1992, ETH Zürich, IV 4/1 – 4/9.
- Kukkamäki, T.J. (1979), Levelling refraction research, its present state and future possibilities, *Proceedings IAU symposium Refractional Influences in Astrometry and Geodesy* (ed. E. Tengström and G. Teleki), Springer, Berlin, Heidelberg, 293 – 299.
- Leica, (2003), TPS Info – Kalibrierung – 01/2003, *Leica Geosystems*, Herbrugg, Switzerland.
- Lewis, J.P. (1995), Fast Template Matching. *Vision Interface 95*, Canadian Image Processing and Pattern Recognition Society, Quebec City, Canada, May 15-19, 1995, 120– 123.
- Mavridis, L.N. and A.L. Papadimitriou (1973), Study of terrestrial refraction in the area of Thessaloniki. *Journal Geophysical Research*, 78(15), 2679 – 2684.
- Ramsayer, K. (1979), The accuracy of the determination of terrestrial refraction from reciprocal zenith angles, *Proceedings IAU symposium Refractional Influences in Astrometry and Geodesy* (ed. E. Tengström and G. Teleki), Springer, Berlin, Heidelberg, 203-212.
- Seeber, G. (2003), Satellite Geodesy, Second Edition, *W. de Gruyter*, Berlin, New York.
- Schofield, W. and M. Breach (2007), Engineering Surveying – 6th Edition, *Butterworth-Heinemann*, Oxford.
- Stober, M. (1995), Untersuchungen zum Refraktionseinfluss bei der trigonometrischen Höhenmessung auf dem grönländischen Inlandeis, In: Festschrift für Heinz Draheim, Eugen Kuntz und Hermann Mälzer, *Geodätisches Institut der Universität Karlsruhe (TH)*, 259 – 272.
- Thomas, M.E., and R.I. Joseph (1996). Astronomical Refraction. *Johns Hopkins APL Technical Digest*, 17(3), The Johns Hopkins University, 279 – 284.
- Torge, W. (2001). Geodesy, third edition. *Walter de Gruyter*, Berlin, New York.
- Tsoulis, D., S. Petrovic, and N. Kilian (2008), Theoretical and numerical aspects of the geodetic method for determining the atmospheric refraction coefficient using simultaneous and mutual zenith observations, *Journal Surveying Engineering* 134(1), 3 – 12.
- Wasmeier, P. (2009), Grundlagen der Deformationsbestimmung mit Messdaten bildgebender Tachymeter, *Deutsche Geodätische Kommission*, C 638, München.
- Webb, E.K. (1984), Temperature and Humidity Structure in the Lower Atmosphere. In: *Geodetic Refraction* (ed. F. Brunner), 85 – 132.
- Weiss, A.I., M. Hennes, and M.W. Rotach (2001), Derivation of the refractive index and temperature gradients from optical scintillometry to correct atmospherically induced errors for highly precise geodetic measurements, *Surveys in Geophysics* 22, 589 – 596.
- Wilhelm, W. (1994), Die Seitenrefraktion. Ein unbeliebtes Thema? Oder ein Thema nur für Insider? *Vermessung, Photogrammetrie, Kulturtechnik*, 2/94, 75 – 82.
- Witte, B. And H. Schmidt (2006), Vermessungskunde und Grundlagen der Statistik im Bauwesen, *Konrad Wittwer Verlag*, Stuttgart, Germany.
- Wunderlich, T. (1985), Die voraussetzungsfree Bestimmung von Refraktionswinkeln. *Geowissenschaftliche Mitteilungen Heft 26*, Technische Universität Wien.
- Young, A.T. (2006), Understanding astronomical refraction, *The Observatory*, 126, 82 – 115, URL: <http://www.ulo.ucl.ac.uk/obsmag/> (accessed 08.02.2010).
- Zeiske, K. (1999), Eine neue Tachymetergeneration von Leica Geosystems, White Paper, *Leica Geosystems*, Herbrugg, Switzerland, 8 pages.

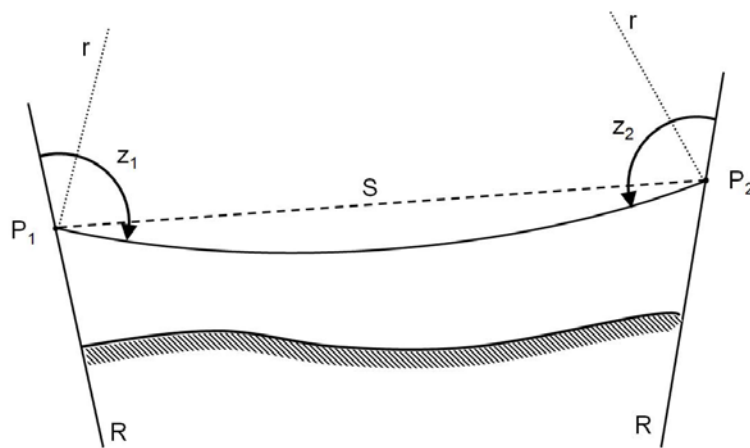


Figure 1. Measurement principle. z_1, z_2 vertical angle measurements, S distance between endpoints, R Earth radius, r refraction radius. Note: the path of light is bent towards the ground (negative refraction coefficient k) which is a typical situation for observations near the surface in summer. Dashed line shows unrefracted sighting between P_1 and P_2

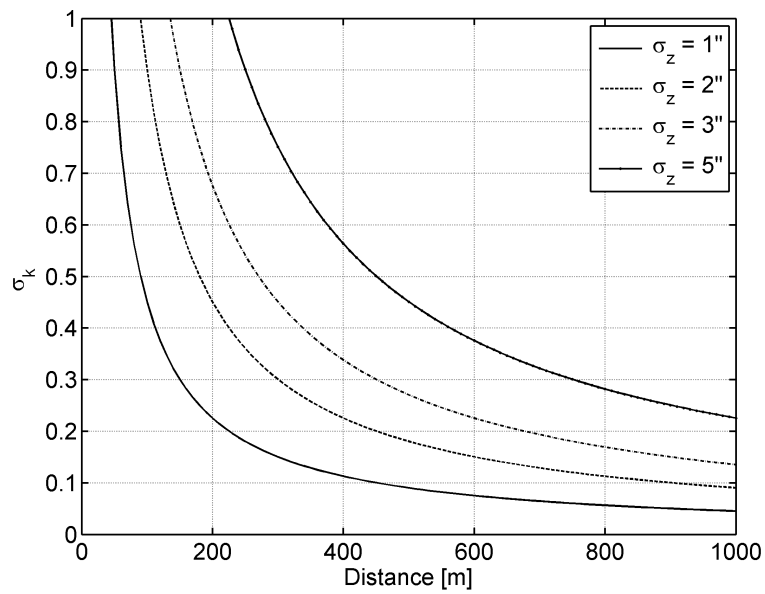


Figure 2. Standard deviation σ_k of the refraction coefficient as a function of the vertical angle accuracy σ_v and distance S between the stations

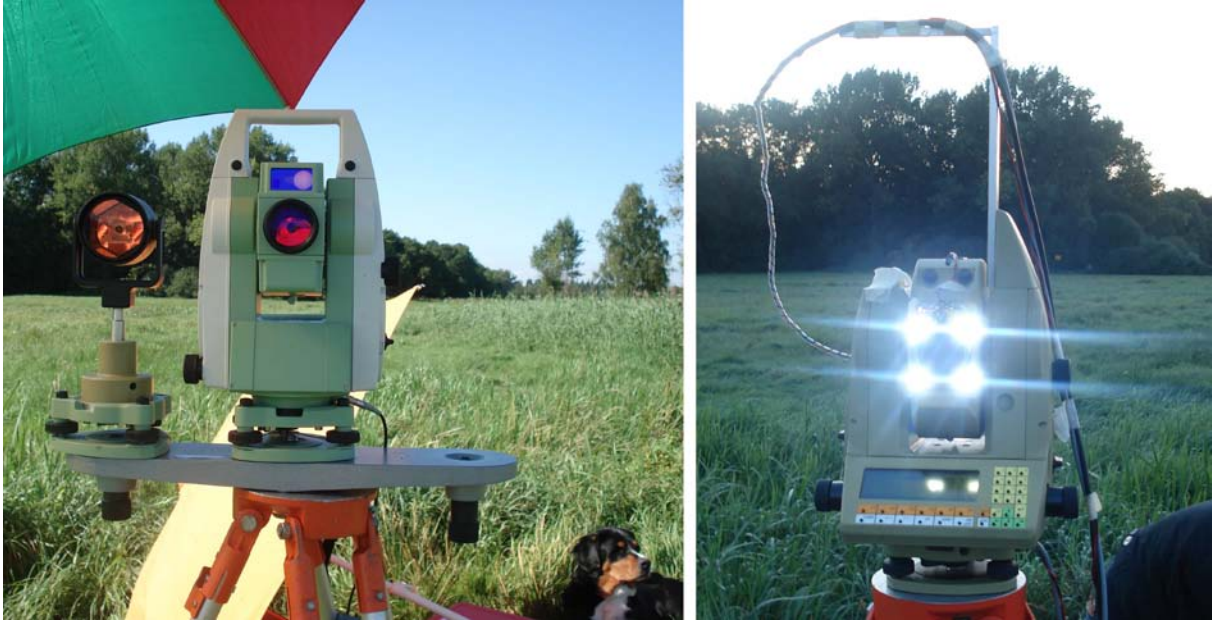


Figure 3. Leica TCRP 1201+ Tachymeter mounted together with retro-reflector on a ground plate (left). Measurement system Daedalus: Leica TCA 1800 equipped with LED target centred to the telescope (right)

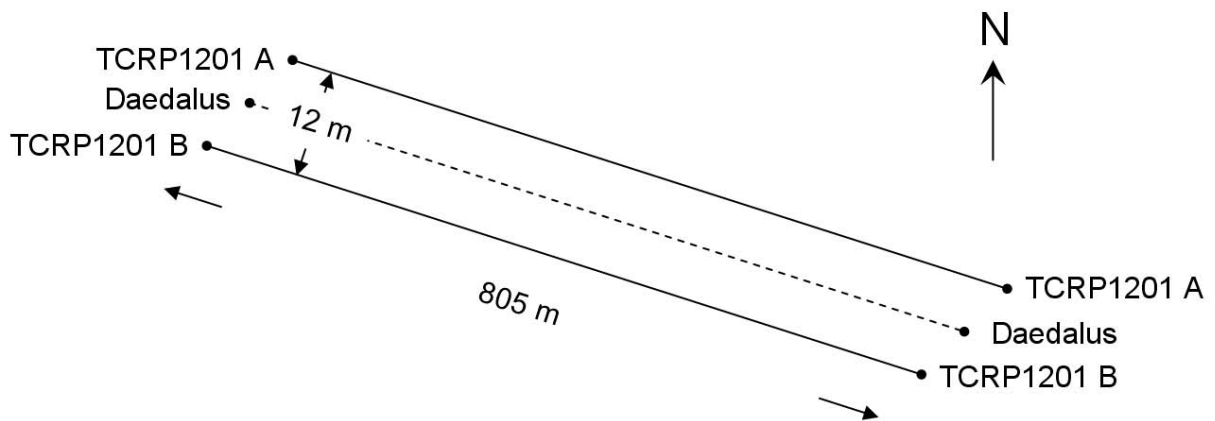


Figure 4. Arrangement of total stations for refraction measurement in test area Grossmoor

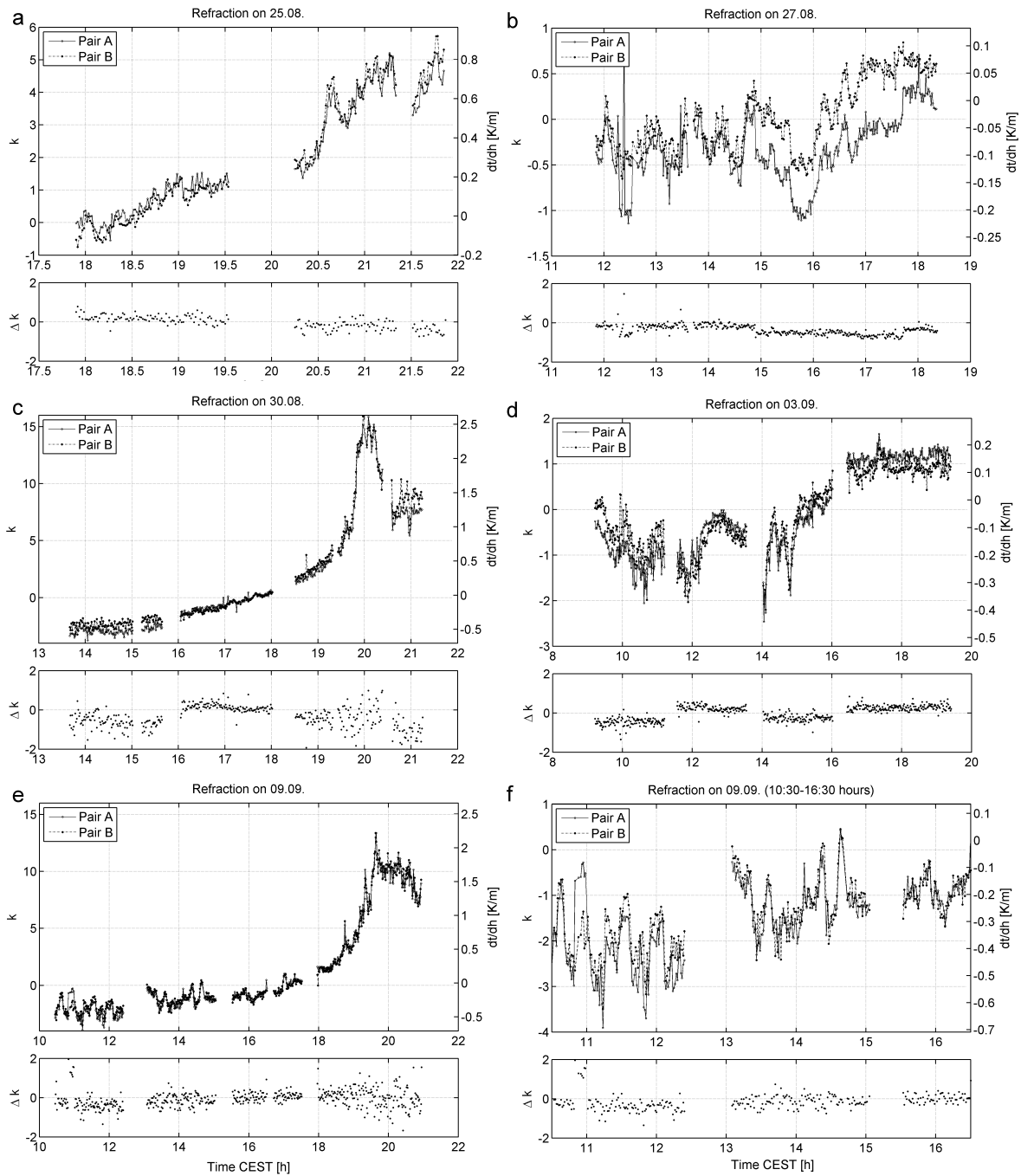


Figure 5. Complete results of refraction measurements using two pairs of TCRP total stations over five days 25.08.08, 27.08.08, 03.09.08 and (cloudy days) and 30.08.08, 09.09.08 (sunny days) along line of sights A and B. The bottom part of each panel shows the differences $\Delta k = k(\text{TCRP A}) - k(\text{TCRP B})$

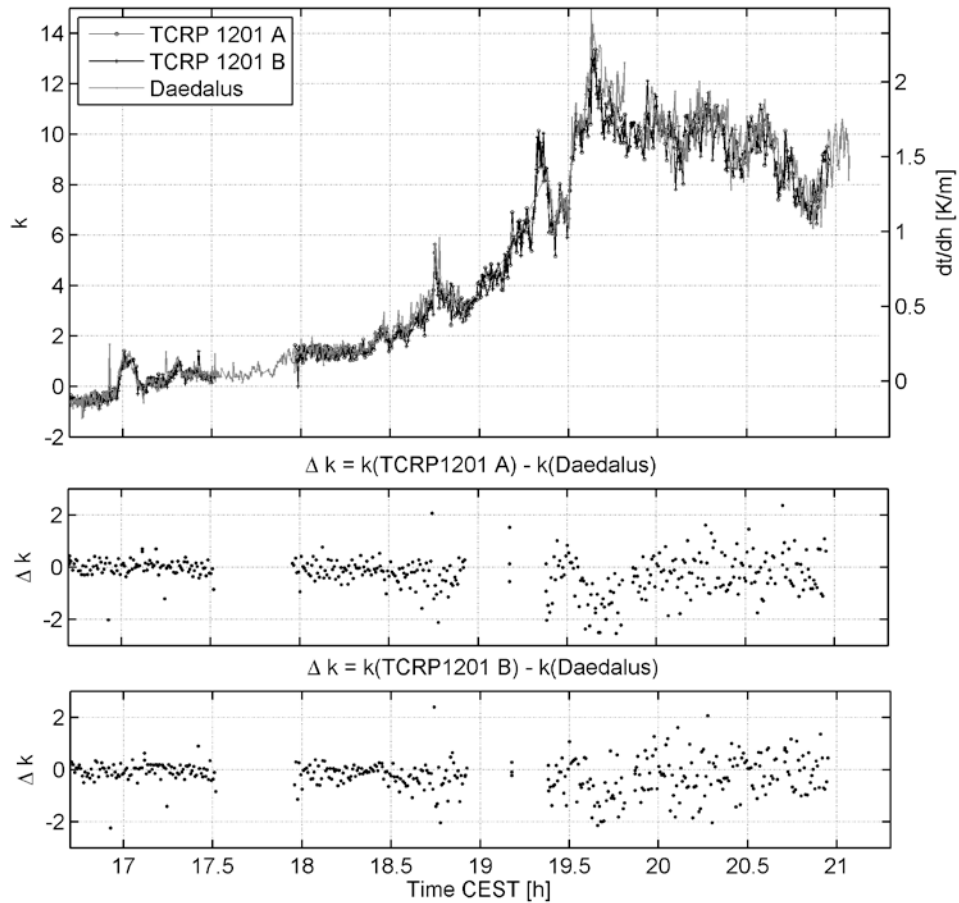


Figure 6. Top: Refraction coefficients k as observed with three pairs of tachymeters (TCRP1201 A, TCRP1201 B and Daedalus) on 09.09.2008. Middle: differences $\Delta k = k(\text{TCRP A}) - k(\text{Daedalus})$, Bottom: differences $\Delta k = k(\text{TCRP1201 B}) - k(\text{Daedalus})$

Table 1. Characteristics of the refraction measurements using Leica TCRP 1201+ and observation system Daedalus

Day	Weather	Temperature [° C]	Instruments	Start [h]	End [h]	Net time [h]	Collected epochs
080825	mostly cloudy	17-20	2x2 TCRP	17.9	21.9	3.1	186
080827	rainy	17-20	2x2 TCRP	11.9	18.4	6.2	373
080830	mostly sunny	14-23	2x2 TCRP	13.7	21.3	6.2	369
080903	cloudy	14-19	2x2 TCRP	9.2	19.4	9.0	538
080909	mostly sunny	20-25	2x2 TCRP	10.5	21.0	8.7	521
080909	mostly sunny	20-25	Daedalus	16.7	21.1	3.9	1014

Table 2. Descriptive statistics of the differences $\Delta k = k(\text{TCRP A}) - k(\text{Daedalus})$, and $\Delta k = k(\text{TCRP B}) - k(\text{Daedalus})$, based on the data collected on 09.09.2008 from 16.7 h to 21.0 h. Daedalus epochs were interpolated to match the TCRP 120 measurement epochs

Δk -difference	Interval [h]	Min	Max	Mean	RMS	STD
TCRP1201 A – Daedalus	16.7-21.0	-2.54	2.37	-0.22	0.70	0.50
	16.7-19.0	-2.11	2.07	-0.11	0.44	0.31
	19.2-21.0	-2.54	2.37	-0.36	0.91	0.64
TCRP1201 B – Daedalus	16.7-21.0	-2.23	2.40	-0.20	0.65	0.46
	16.7-19.0	-2.23	2.40	-0.14	0.46	0.32

	19.2-21.0	-2.13	2.06	-0.26	0.83	0.58
--	-----------	-------	------	-------	------	------

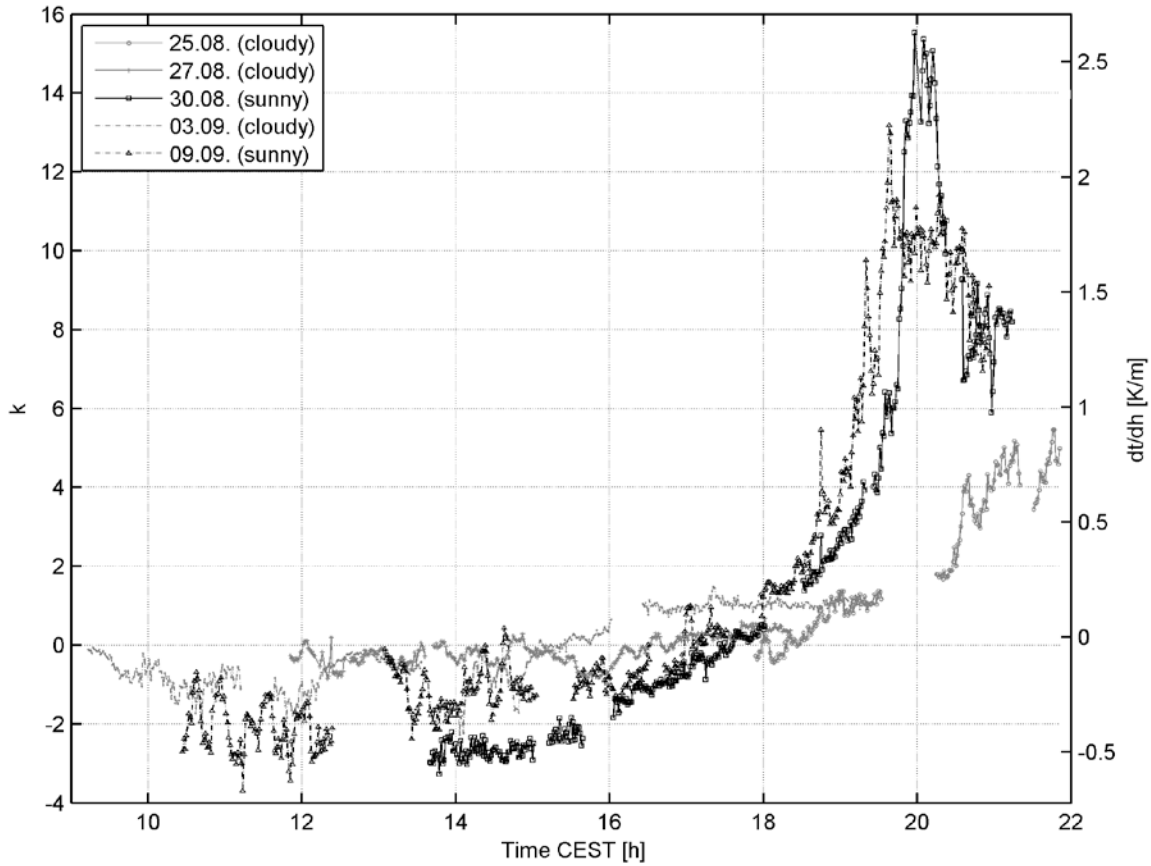


Figure 7. Refraction coefficients k on cloudy days (25.08.08, 27.08.08 and 03.09.08) and sunny days (30.08.08 and 09.09.08). The displayed data are average values as observed along lines of sight A and B

Table 3. Descriptive statistics of the differences $\Delta k = k(\text{TCRP A}) - k(\text{TCRP B})$. $\text{STD} = \text{RMS}/\sqrt{2}$, assuming both k -values to have the same precision

Day	Min	Max	Mean	RMS	STD
080825	-0.78	0.74	0.02	0.31	0.22
080827	-1.47	0.84	0.36	0.44	0.31
080830	-0.98	3.36	0.38	0.71	0.50
080903	-0.84	1.36	0.02	0.36	0.25
080909	-1.96	1.68	0.06	0.45	0.31

Table 4. Descriptive statistics of the de-biased $k \Delta k = k(\text{TCRP A}) - k(\text{TCRP B})$. $\text{STD} = \text{RMS}/\sqrt{2}$, assuming both k -values to have the same precision. Note: The bias (mean value) of the differences of each measurement session is removed

Day	Min	Max	Mean	RMS	STD
080825	-0.61	0.64	0.00	0.22	0.15
080827	-1.66	0.51	0.00	0.23	0.16
080830	-1.62	2.10	0.00	0.41	0.29
080903	-0.64	0.89	0.00	0.17	0.12
080909	-2.22	1.69	0.00	0.42	0.30